

Direct photons in d+Au collisions at $\sqrt{s_{NN}} = 200$ GeV with STAR

M J Russcher for the STAR collaboration

Utrecht University, Utrecht, The Netherlands
e-mail: m.j.russcher@phys.uu.nl

Received: date / Revised version: date

Abstract. Results are presented of an ongoing analysis of direct photon production in $\sqrt{s_{NN}} = 200$ GeV deuteron-gold collisions (d+Au) with the STAR experiment at RHIC. A significant excess of direct photons is observed near mid-rapidity ($0 < y < 1$) and found to be consistent with next-to-leading order pQCD calculations including the contribution from fragmentation photons.

PACS. 25.75.-q Relativistic heavy-ion collisions

1 Introduction

Direct photons are an interesting tool to study the quark-gluon plasma (QGP) created in ultra-relativistic heavy-ion collisions [1]. These photons are directly produced in processes like quark-anti-quark annihilation ($q+\bar{q} \rightarrow g+\gamma$) and quark-gluon Compton scattering ($q+g \rightarrow q+\gamma$) and do not originate from hadronic decays. Their main advantage is that they do not interact with the color charges when traversing the dense medium that is formed in the heavy-ion collision.

It is expected that thermal photons dominate the direct photon yield at low transverse momentum (p_T). Since the thermal photon spectrum falls off exponentially with p_T , the prompt photons from the initial hard (pQCD-like) scattering will dominate the spectrum at higher p_T , as can be seen from the calculation shown in Figure 1. In addition there is a contribution from photons produced during the fragmentation of the partons. The yield of these photons can be determined using parton-to-photon fragmentation functions [3].

The thermal photons are radiated by the electric charges in the QGP and the hadron gas which is formed in the later stage of the expansion. Their momentum distribution is therefore a measure for the temperature of both phases [2]. A measurement of thermal photons can thus provide information on the temperature evolution of the system.

The measurement of prompt photons is of interest, first of all because they form a background to the measurement of the thermal component. Furthermore, events with a tagged prompt photon and a recoil jet are a promising tool to study the interaction of the jet with the medium [4].

The production of high p_T particles in nucleus-nucleus (A+A) collisions is often represented by the nuclear mod-

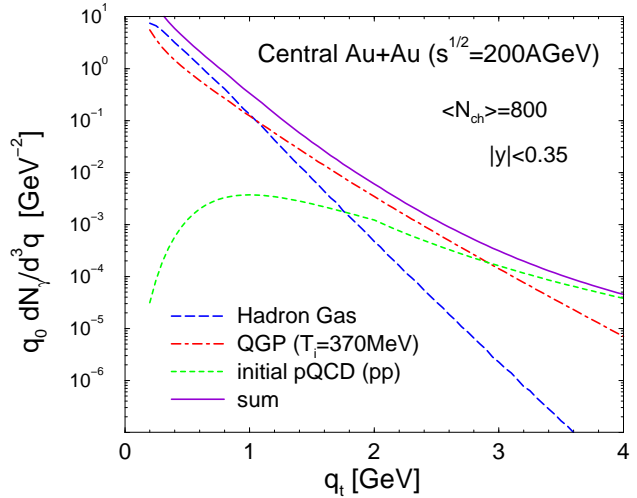


Fig. 1. Theoretical calculation for the mid-rapidity direct photon yield in central Au+Au collisions at RHIC as a function of transverse momentum (q_t), coming from various sources. (figure from [2])

ification factor

$$R_{AA} = \frac{dN^{AA}/dp_T}{\langle N_{bin} \rangle dN^{pp}/dp_T} \quad (1)$$

which is the yield of hadrons in A+A collisions relative to a scaled reference spectrum measured in proton-proton (p+p) collisions. The scale factor $\langle N_{bin} \rangle$ is the number of binary nucleon-nucleon collisions which can be calculated in the framework of a Glauber-model. For sufficiently hard (high p_T) processes it is expected that particle production scales with $\langle N_{bin} \rangle$. However, a suppression of hadrons by a factor of 5 was observed [5, 6, 7, 8] and has been attributed to in-medium parton energy loss.

Prompt photons provide a way to test binary collision scaling since their production is not affected by the medium produced in the final state of the interaction. A recent measurement at RHIC indeed shows that high p_T direct photon production in gold-gold (Au+Au) interactions is consistent with $\langle N_{bin} \rangle$ scaling ($R_{AA} \sim 1$) [9].

At RHIC there is the possibility to study direct photon production not only in Au+Au, but also in p+p and d+Au collisions. Direct photon production in p+p collisions can serve as a high precision test of pQCD, while in d+Au collisions it can be used to investigate nuclear effects such as the existence of a Color Glass Condensate [10, 11] and multiple rescattering (Cronin enhancement) [12]. However, the measurement of direct photons, be it in p+p, d+Au or Au+Au collisions, will always be challenging because of the large background of photons from hadronic decays.

2 Experiment

The data presented here were taken with the STAR detector [13] in the $\sqrt{s_{NN}} = 200$ GeV d+Au run at RHIC. A minimum bias trigger was provided by requiring a signal over threshold in the Zero Degree Calorimeter (ZDC) in the Au beam direction (at negative pseudorapidity).

The energy of the photon showers was measured with the Barrel Electromagnetic Calorimeter (BEMC) [14] consisting of 4800 lead-scintillator cells with a spatial granularity of $\Delta\eta \times \Delta\phi = 0.05 \times 0.05$. The BEMC is positioned at a distance of 2.3 m from the beam axis and covers full azimuth in the pseudorapidity interval $|\eta| < 1$. During the d+Au run however, only half of the detector ($0 < \eta < 1$) was instrumented. The absolute energy scale of the BEMC was calibrated to a precision of 5% using minimum ionizing particles and electrons reconstructed in the Time Projection Chamber (TPC) [15].

A gaseous wire-proportional counter with strip readout is located inside the BEMC at a depth of 5–7 radiation lengths [14]. The finer segmentation ($\Delta\eta \times \Delta\phi = 0.007 \times 0.007$) of this Barrel Shower Maximum Detector (BSMD) allows to measure the transverse profile of the showers and makes it possible to resolve the two π^0 decay photons in the high p_T region.

To enhance the particle yield at high p_T , a level-0 trigger selected events with a high transverse energy deposition in a single BEMC cell. The integrated luminosity, after all event cuts, is $105 \mu\text{b}^{-1}$ and $996 \mu\text{b}^{-1}$ associated with an effective p_T threshold set at 2.5 and 4.5 GeV, respectively.

3 Analysis

This analysis aims to measure the direct photon yield in d+Au collisions by means of a statistical subtraction of the hadronic decay background from the measured inclusive photon spectrum. The dominant contribution to this background is from the decay $\pi^0 \rightarrow \gamma\gamma$. Therefore it is

Table 1. Dominant meson decay contributions to the inclusive photon yield. The factor used for scaling the transverse mass spectra (see text) is given in the last column.

decay	branching ratio	m_T -scale
$\pi^0 \rightarrow \gamma\gamma$	98.80%	N/A
$\pi^0 \rightarrow e^+e^-\gamma$	1.20%	
$\eta \rightarrow \gamma\gamma$	39.23%	0.45
$\eta \rightarrow \pi^+\pi^-\gamma$	4.78%	
$\eta \rightarrow e^+e^-\gamma$	0.49%	
$\omega(782) \rightarrow \pi^0\gamma$	8.69%	1.0

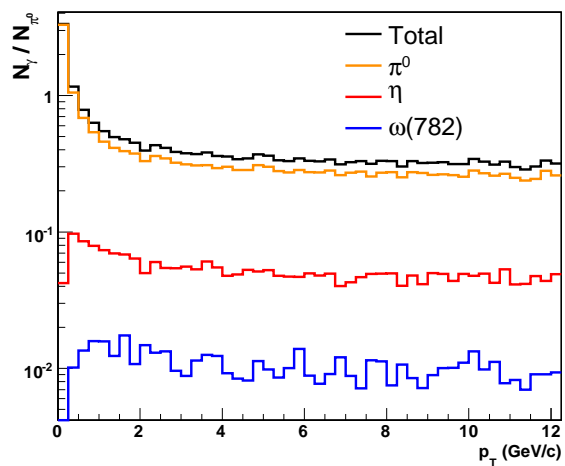


Fig. 2. The number of photons per input pion N_γ/N_{π^0} from hadronic decays versus p_T , obtained from a simulation described in the text.

important to constrain the π^0 yield with high precision. This yield has been determined in an earlier analysis of the present data as reported in [16].

The total photon yield from hadronic decays, see Table 1, was simulated with a Monte-Carlo algorithm. Input to this simulation is a fit to the measured π^0 spectrum. Since there are no measurements available of the η and $\omega(782)$ yields, we assume that their transverse mass (m_T) spectra scale with that of the π^0 by a constant factor. In this analysis, these factors were taken to be $\eta/\pi^0 = 0.45 \pm 0.05$ and $\omega/\pi^0 = 1 \pm 0.2$, consistent with measurements reported in [17] and [18]. The other possible contributions to the hadronic decay background were found to be negligible. In figure 2 we show the p_T dependence of the decay photons, normalized to the generated π^0 spectrum.

In this analysis, inclusive photon candidates were identified by a clustering algorithm based on the energy measured in the BEMC and on the shower profile measured in the BSMD. To identify neutral clusters and decrease hadronic background, a charged particle veto (CPV) is provided by rejecting clusters with a pointing TPC track.

The raw inclusive photon yield has been corrected for (anti-)neutron contamination by means of a GEANT sim-

ulation of the detector, which had the measured proton and anti-proton spectra as an input [19]. Correction factors to account for reconstruction and trigger efficiency, limited acceptance, photon conversions in the detector material and the inefficiency of the CPV were determined from an analysis of GEANT hits embedded in real d+Au data.

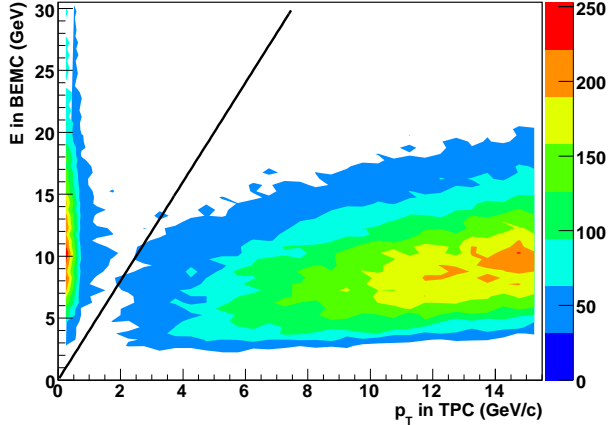


Fig. 3. The energy deposited in the BEMC versus the total momentum of charged tracks, reconstructed with the TPC. There is a sizeable contribution of events which have a large amount of energy in the BEMC but very little TPC momentum. The full line shows the cut that was used to exclude these events from the analysis.

A prominent background to the measurement is due to scattering of the deuteron beam halo on material located upstream of the STAR interaction region. Such events are characterized by a large deposition of energy in the BEMC without associated tracks reconstructed in the TPC and thus do have the signature of a collection of neutral clusters. A cut on the ratio of the TPC momentum to the BEMC energy was used to remove these events from the data sample, see Figure 3.

4 Results

To determine the direct photon yield we have calculated the double ratio

$$R = \frac{(\gamma/\pi^0)_{measured}}{(\gamma/\pi^0)_{decay}} = 1 + \frac{\gamma_{direct}}{\gamma_{decay}} \quad (2)$$

where the numerator is the point by point ratio of the measured inclusive photon spectrum to the neutral pion spectrum and the denominator is the number of simulated decay photons per input pion as shown in Figure 2. It is clear that many systematic uncertainties, which are common to neutral pion and inclusive photon detection will (partially) cancel in this ratio. The remaining uncertainties in the ratio R are listed in Table 2.

Table 2. Dominant contributions to the systematic error on the ratio R defined in equation 2 for two p_T bins at 3 and 10 GeV/ c .

$(\gamma/\pi^0)_{meas}/(\gamma/\pi^0)_{bg}$	3 GeV/ c	10 GeV/ c
pion yield extraction	5%	10%
reconstruction efficiency (stat.)	10%	4.5%
BSMD gain uncertainty	5%	5%
beam background	< 1%	4%
BEMC energy scale	3%	3%
$\eta/\pi^0 = 0.45 \pm 0.05$	3%	3%

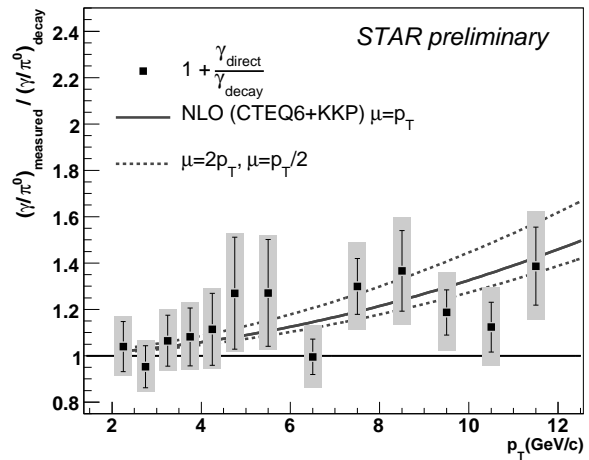


Fig. 4. The double ratio R , defined in equation 2, as a function of p_T . The error bars (grey boxes) indicate the statistical (total) error on the data points as specified in Table 2. The full line is a pQCD calculation for p+p collisions using the CTEQ6M parton densities and KKP fragmentation functions. The dashed lines show the sensitivity of the calculation to the factorization scale.

In Figure 4 we show the p_T dependence of R obtained from the d+Au data set. The significant excess above unity at large p_T indicates the presence of a direct photon signal. The double ratio is consistent with a pQCD calculation [20] based on the CTEQ6M parton density functions [21] and KKP fragmentation functions [22] as shown for three different factorization scales by the curves in Figure 4. Since this analysis does not make use of an isolation cut the calculated direct photon yield includes both prompt and fragmentation photons.

5 Outlook

The significance of the measurement will be much improved by reducing the error contribution from the BSMD which has not been calibrated in-situ so far. In addition, dedicated TPC tracking algorithms and BEMC pattern recognition algorithms are presently being developed to better identify beam-background events which will reduce the systematic uncertainty from this source and the sta-

tistical error on the efficiency correction is also being improved.

The direct photon analysis of the 2005 p+p data set is in progress. The combined d+Au and p+p results will provide insight into nuclear effects and constitute a necessary baseline to study the properties of the QGP from direct photon measurements in Au+Au collisions.

References

1. Peitzmann T and Thoma M H 2002 *Phys. Rept.* **346** 175
2. Turbide S *et al* 2004 *Phys. Rev. C* **69** 014903
3. Bourhis L *et al* 1998 *Eur.Phys.J. C* **2** 529
4. Wang X N *et al* 1996 *Phys. Rev. Lett.* **77** 231
5. Arsene I *et al* 2003 *Phys. Rev. Lett.* **91** 072305
6. Adler S S *et al* 2003 *Phys. Rev. Lett.* **91** 072303
7. Back B B *et al* 2003 *Phys. Rev. Lett.* **91** 072302
8. Adams J *et al* 2003 *Phys. Rev. Lett.* **91** 072304
9. Adler S S *et al* 2005 *Phys. Rev. Lett.* **91** 232301
10. Iancu I *et al* 2001 *Nucl. Phys. A* **692** 583
11. Ferreira E *et al* 2002 *Nucl. Phys. A* **703** 489
12. Cronin J *et al* 1975 *Phys. Rev. D* **11** 3105
13. Ackermann K H *et al* 2003 *Nucl. Instrum. Meth. A* **499** 624
14. Beddo M *et al* 2003 *Nucl. Instrum. Meth. A* **499** 725
15. Anderson M *et al* 2003 *Nucl. Instrum. Meth. A* **499** 659
16. Mischke A *et al* 2005 *Eur. Phys. J. C* **43** 311
17. Adler S S *et al* 2006 *Phys. Rev. Lett.* **96** 202301
18. Diakonou M *et al* 1980 *Phys. Lett. B* **89** 432
19. Adams J *et al* 2006 *Phys. Lett. B* **637** 161
20. Vogelsang W 2006 *private communication*
21. Pumplin J *et al* 2002 *J. High Energy Phys.* **07** 012
22. Kniehl B A *et al* 2001 *Nucl. Phys. B* **597** 337